(Received 11 September 2023, Accepted 17 November 2023, Scheduled 24 November 2023)

Research on Anti-Offset Performance of the Wireless Power Transfer System with Asymmetric Coupling System

Xiangyang Shi, Jianwei Kang*, Deyu Zeng, and Yang Shi

Key Laboratory of Testing Technology for Manufacturing Process, Ministry of Education
School of Manufacturing Science and Engineering, Southwest University of Science and Technology, Mianyang 621010, China

ABSTRACT: Coupling system is important for a Wireless Power Transfer (WPT) system, and it directly affects the efficiency and reliability of the WPT system. In some special applications, such as implantable medical devices, the size of the receiving coil of the WPT system is strictly limited. Coupling coils of equal size will not meet the application requirements. When being applied in implantable medical devices, equal-size coupling coils suffer from shortcomings such as poor anti-offset performance and cumbersome design process. In view of the above problems, in this paper we design a coupled coil structure asymmetrically, so that parameters such as outer diameter and the number of turns of the transmitting and receiving coils are no longer equal. In this paper, we first analyze the effect of tightly wound and loosely wound coils on the WPT system when they are used separately as transmitting coils and find that the two different types of coils have different characteristics of the magnetic induction intensity distribution. Then, we use the genetic algorithm to optimize the transmission coil and design a new asymmetric coupling system. Finally, we experimentally demonstrate that the optimized coupling system is able to maintain the stability of the output current and the transmission efficiency within a certain range in the presence of offset, which indicates that the coupling system has a certain ability of anti-offset.

1. INTRODUCTION

Wireless power transfer (WPT) is a new type of power transmission method in which the load and power supply are without contact, which has the advantages of safety, flexibility, and reliability compared with the traditional transmission methods [1–6]. WPT has a broad application in the fields of implantable medical devices [7, 8], electric vehicles [9, 10], etc.

Coupling system is an important component of a WPT system. Its parameters such as coupling coefficient and mutual inductance coefficient directly affect the transmission power and efficiency of the WPT system [11]. However, the mutual inductance coefficient is affected by many factors such as coil structure and the relative position of coils [12], which makes the design and optimization of a coupling system a great challenge. Especially in the case of implantable medical devices, the receiving coils are subject to strict size limitations. Conventional equal-size coil systems, where the transmitting and receiving coils are of equal size, no longer meet the requirements in implantable devices. Moreover, since the implantable WPT system cannot be aligned with the coil by visual judgment, the ability to anti-offset the coupling system is highly desired.

At present, numerous scholars have carried out research on the problem of anti-offset coil and the asymmetric coil of a coupling system for special WPT situations. The anti-offset coil of the conventional dual-coil structure is usually optimized by turn spacing, coil outer diameter, or wire diameter [13, 14]. Besides, triple-coil [15, 16], quadruple-coil [17] structures, and the coil structures with magnetic cores also improve the ability of anti-offset to some extent. In recent years, the design of a anti-offset coil is no longer limited to conventional structures, and the researchers at the University of Auckland have proposed a different structure of coupling coils, which is an orthogonal double-D structure [18], improving the lateral offset resistance of the coils. A spherical coil is proposed by the researchers of Wuhan University [19], which realizes the multi-directional transmission of electric energy and effectively improves the weakness of traditional WPT system's poor anti-offset ability. In addition, with the deepening of research, some researchers use intelligent algorithms to optimize the structure of WPT coil, such as genetic algorithm (GA) and particle swarm optimization (PSO) [20, 21]. With the help of intelligent optimization algorithm, many new structures, such as combined series wound coil structure [22], are proposed, which provides a new research idea for improving the anti-offset ability of WPT system.

The above mentioned studies have implemented anti-offset by optimizing the coil structure, and there are two main optimization methods: finite element methods and analytical methods. The finite element method mainly uses software to calculate the electromagnetic field in the WPT system. Its advantage is that it is easy to operate, but the calculation of the load model requires a large amount of computational resources [23], while the analytical method uses the electromagnetic field theory to construct the mutual inductance model between the coils, and the method analyzes the results under different working conditions. The analytical method possesses a clear physical significance [24], but it brings some cumbersome formulas. However, depending on the specific problem, both methods can be used in optimization.

* Corresponding authors: Jianwei Kang (kjw689@163.com).

In this paper, we present a study of a novel asymmetric coil for WPT systems based on the GA method. The proposed coil system has good anti-offset ability and can be used in some special cases, such as implantable medical devices. Firstly, the restricted receiving coil size is confirmed by analyzing the relationship between the transmission efficiency of the WPT system and asymmetric coupling system. Secondly, the system parameters are analyzed by the finite element method under the coil offset condition. Thirdly, the coil parameters are optimized through the GA optimization algorithm in order to enhance its stability under the offset condition. At last, an experiment is conducted to verify the proposed coil system and the optimization method.

2. ANALYSIS OF THE ASYMMETRIC COUPLING SYSTEM IN A WPT SYSTEM

2.1. The Asymmetric Coupling System Circuit

A magnetically coupled resonant wireless power transfer (MCR-WPT) system is shown in Figure 1. The system consists of a high-frequency inverter power supply, a matching network, an asymmetric coupling coil, a rectifier circuit, and a load. The circle on the primary side represents the transmitting coil, and the circle on the secondary side represents the receiving coil. The sizes of the two coils are not equal, which is consistent with special WPT cases such as the implantable medical device case.

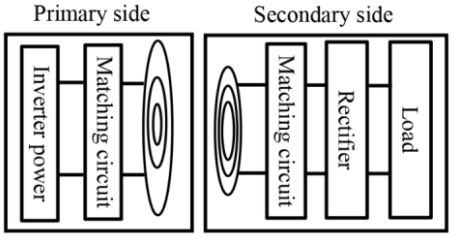

FIGURE 1. The system block diagram of MCR-WPT.

Figure 2 shows the equivalent circuit of the system using an S-S type topology compensation circuit. Here, u_s is the high-frequency excitation voltage source. C_1 and C_2 are the series compensation resonant capacitances of the transmitting coil and the receiving coil. R_1 and R_2 are the sum of the AC loss resistance and the coil reflection resistance of the transmitting and receiving coils. L_1 and L_2 are the equivalent inductance of the transmitting coil and receiving coil of the two series coils. M_{12} is the mutual inductance between the two coils, and R_L is the load resistance.

Assuming that the operating frequency of the system is ω, the equivalent impedance of the transmitter and receiver side loops is:

$$\begin{cases} Z_1 = R_1 + j\omega L_1 + \dfrac{1}{j\omega C_1} \\ Z_2 = R_2 + j\omega L_2 + \dfrac{1}{j\omega C_2} + R_L \end{cases} \tag{1}$$

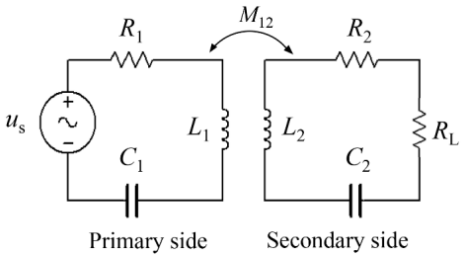

FIGURE 2. The equivalent circuit of the coil system.

When the system is in a resonant state, and the impedance imaginary part is zero, the maximum transmission efficiency of the system is:

$$\eta = \frac{p_{out}}{p_{in}} = \frac{(\omega M_{12})^2 R_L}{(R_{_L} + R_2)[R_1(R_L + R_2) + (\omega M_{12})^2]} \times 100\% \tag{2}$$

Eq. (2) shows that the efficiency η is closely related to parameters load size, internal resistance between transmitting coil and receiving coil, frequency, and mutual inductance. The efficiency of the WPT system is one of the key optimization objectives when coil systems are optimized.

2.2. Mutual Inductance Model of the Asymmetric Coupling System

The asymmetric coupling system is shown in Figure 3, where d is the axial distance between the two coils, and t is the radial distance between the two coils.

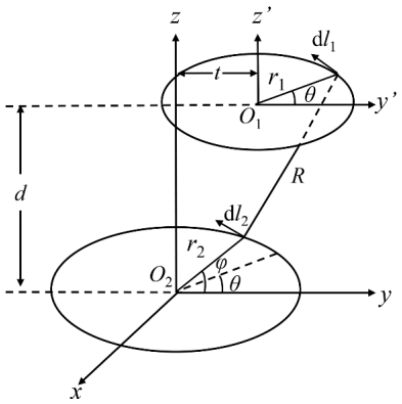

FIGURE 3. Model of an asymmetric coupling system.

In Figure 3, the coordinates of O_1 are (0, t, d), and the coordinates of O_2 are (0, 0, 0). When the two coils have a radial offset, the mutual inductance between the two coils [25] is:

$$M = \frac{\mu_0 N_1 N_2}{4\pi} \int_0^{2\pi} \int_0^{2\pi} \frac{r_1 r_2 \cos(\theta - \varphi) d\theta d\varphi}{R} \tag{3}$$

where N_1 and N_2 are the number of turns of the transmitting coil and the receiving coil; d and t are the axial distance and radial distance of the two coils; r_1 and r_2 are the radii of the two coils; θ and φ are the angles between dl_1 and dl_2 and the x axis, respectively.

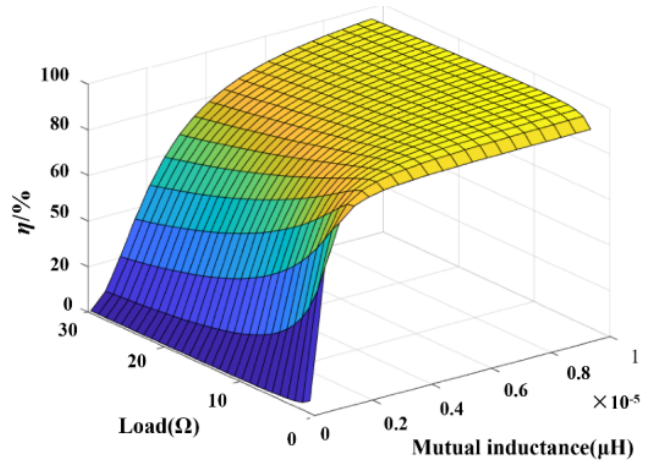

FIGURE 4. The efficiency influenced by the load resistance and the mutual inductance.

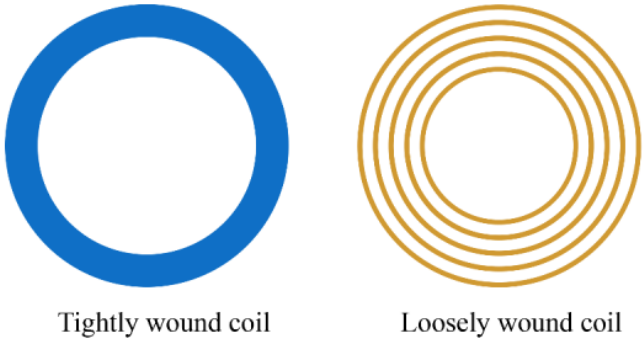

FIGURE 5. Two different types of coils.

TABLE 1. Parameters of the coupling system.

Parameters	Tightly wound coil	Loosely wound coil	Receiving coil
Number of turns	8	13	1
External diameter/mm	160	160	4
Turn spacing/mm		4.3	
Wire diameter/mm	2	2	1
Self-inductance/μH	17.2	17.5	3.6

3. THE SYSTEM CHARACTERISTIC OF THE ASYMMETRIC COUPLING SYSTEM

The WPT efficiency and the transmission power are directly affected by parameters including the load resistance and the mutual inductance, according to Eq. (2), and the magnetic induction intensity is the key of the power transfer, and it is affected by the coil type. Thus, this section analyzes the effect of the above circuit parameters and the winding method of the coil on the WPT system.

3.1. The Influence of Load and Mutual Inductance on Transmission Performance

A 3-D result is calculated by using Matlab in order to visually describe the relation of R_L, M_{12}, and η, shown in Figure 4. For the WPT system of the asymmetric coupling system studied in this paper, the parameters are as follows: the system operating frequency is 1.5 MHz; the transmitting coil inductance $L_1 = 20.5\,\mu\text{H}$; the resistance $R_1 = 0.35\,\Omega$; the receiving coil inductance $L_2 = 6.4\,\mu\text{H}$; the resistance value $R_2 = 0.1\,\Omega$. The range of load R_L is set to $0 \sim 30\,\Omega$, and the range of mutual inductance M_{12} is set to $0 \sim 10\,\mu\text{H}$.

Figure 4 shows that when the load is fixed, the efficiency of the system first increases and then remains constant as the mutual inductance increases, while for small values of the mutual inductance, the efficiency changes significantly with the mutual inductance. The mutual inductance between the coils in asymmetric coupling systems is often small, and coil offsets can have a large effect on the mutual inductance, so it is necessary to maintain the stability of the mutual inductance in asymmetric coupling systems.

3.2. The Influence of the Coil Wound Type

As shown in Figure 5, a conventional circular coil is divided into two types, tightly wound and loosely wound. The difference between the two type coils is that the tightly wound coil has little or no turn spacing, while the loosely wound coil has larger turn spacing.

In order to analyze the influence mechanism of the spatial magnetic induction intensity distribution of the WPT system of the asymmetric coupling system, the two types of circular coils are used as transmitting coils. Then the spatial distribution of magnetic induction intensity of the two different coupling systems is analyzed by using the finite element method. A condition is fixed that the outer diameters of the two types of coils are the same, and the self-inductances are similar to obtain a better comparison. The parameters of the coupling system are given in Table 1, and Figure 6 shows the respective magnetic induction intensity distribution.

According to the simulation results, the spatial magnetic induction intensity of the coupling system is affected by the coil winding approach. The magnetic induction intensity of the tightly wound coil is denser on both sides of the coil and decreases in the coupling area. The magnetic induction intensity of the loosely wound coil is stronger in the central coupling area than that in the outer area of the coil due to the spacing between the wires.

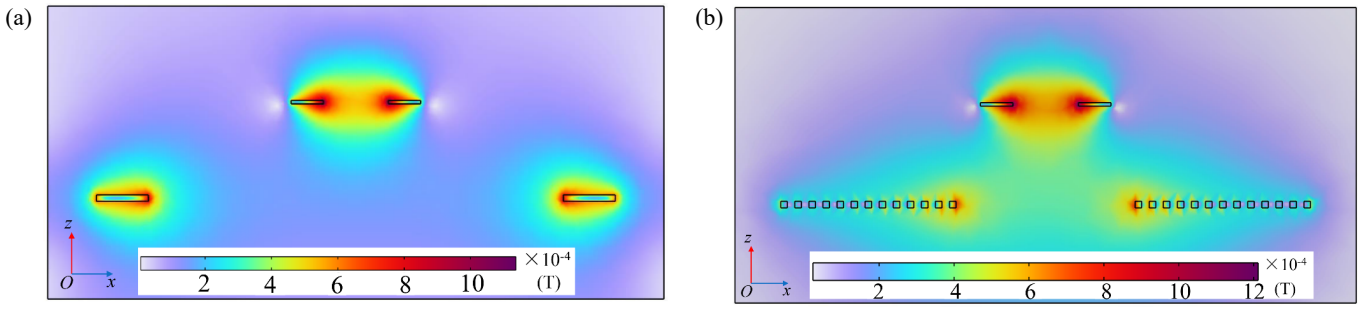

FIGURE 6. Magnetic induction density distribution of two types of coils. (a) Tightly wound coil and (b) Loosely wound coil.

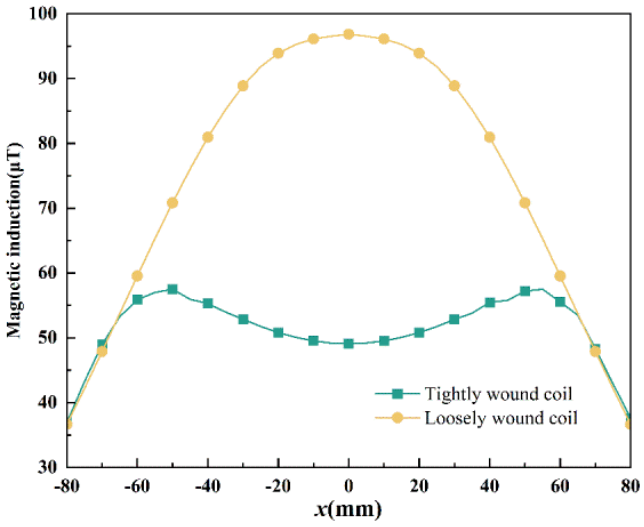

FIGURE 7. Trends in magnetic induction intensity.

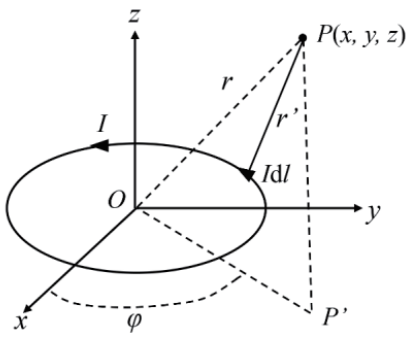

FIGURE 8. Schematic diagram of the ring current.

Figure 7 shows the trend of magnetic induction intensity at 30 mm above the transmitting coil plane. In the range of [−60, 60] mm, the magnetic induction intensity of loosely wound coils is greater than that of tightly wound coils, but the uniformity of tightly wound coils is better than that of loosely wound coils. The mutual inductance of the coupling system and the degree of uniformity of the spatial magnetic field are the key factors in determining the transmission efficiency of the WPT system.

Therefore, inspired by the respective advantages of the above two types of coils, one proposes an optimization method for transmitting coil of the asymmetric coupling system.

4. COIL OPTIMIZATION BASED ON GA

According to the law of electromagnetic induction, only the Z-direction component of the magnetic induction intensity generated by the transmitting coil contributes to the magnetic flux of the receiving coil, so this section will take the uniformity of the Z-direction magnetic induction intensity of the plane where the receiving coil is located as the optimization goal. According to the inspiration of the third section, this section will use GA to adjust the turn spacing of the transmitting coil, so as to achieve the optimal uniformity of magnetic induction intensity in Z-direction.

4.1. Magnetic Field Analysis of Circular Current Loop

Figure 8 shows a ring current and an arbitrary point P (x, y, z) in the space. The radius of the ring current is a; the current passing through is I; the current around is counterclockwise.

Since the magnetic field generated by the ring current is symmetric, the point P can be expressed in a cylindrical coordinate:

$$\begin{cases} x = \rho\cos\varphi \\ y = \rho\sin\varphi \\ z = z \end{cases} \tag{4}$$

where ρ is the distance from the projection of point P on xOy plane to point O, and φ is the included angle between the projection of point P on xOy plane and the connecting line of point O and x axis.

The component of the magnetic induction intensity at point P along z axis [26] is:

$$B_z = \frac{\mu_0}{4\pi}\int_0^{2\pi} \frac{Ia(a-\rho\cos\beta)}{\sqrt{(a^2+\rho^2+z^2-2\rho\cos\beta)}^3}d\beta \tag{5}$$

where a is the radius of annular current, and I is the current passing through.

4.2. Optimization Process and Objective Function

Since the transmitting coil is a multi-turn coil, the magnetic induction intensity at any point in the surrounding space can be obtained by the superposition of the magnetic induction intensity generated at that point by each turn of wire:

$$B_z = \sum_{i=1}^{n} B_{zRi} \tag{6}$$

The position of the transmitting coil and a region to be optimized is shown in Figure 9. The region is the plane where the receiving coil is located. B_z on this plane will be homogenized by GA.

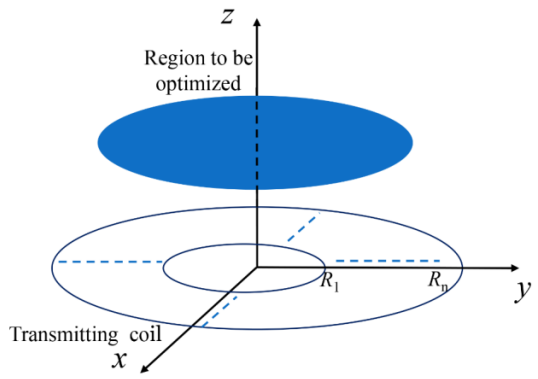

FIGURE 9. Schematic diagram of a disc coil and optimization plane.

Because the transmitting coil and the region to be optimized are both circular, the B_Z in this region is symmetrical. Since the distribution law of magnetic induction intensity on every radius in this region is the same, the problem of magnetic induction intensity homogenization on the plane can be transformed into the problem of magnetic induction intensity optimization on a certain radius.

Based on the above analysis, one takes a certain radius in the region to be optimized as the optimization object, evenly selected points on this radius are shown in Figure 10. Then, the turn pitch of the transmitting coil is optimized by GA to make the B_z of these points as consistent as possible. The schematic diagram of uniform selection points is shown in Figure 10. In the follow-up study, the radius of the region to be optimized is set to 40 mm, so 20 points on one radius will be considered.

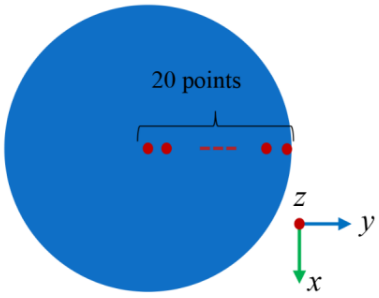

FIGURE 10. Schematic diagram of uniform selection points.

An objective function represents the degree of the uniformity of the magnetic inductance intensity, and the objective function is defined as the Coefficient of Variance (COV):

$$\mathrm{COV} = \frac{\sqrt{\frac{1}{n}\left[\sum_{i=1}^{n}\left(B_{zi} - \frac{1}{n}\sum_{i=1}^{n} B_{zi}\right)^2\right]}}{\frac{1}{n}\left|\sum_{i=1}^{n} B_{zi}\right|} \tag{7}$$

where n is the number of points on the radius of the optimization region, and B_{zi} is the z-axis direction magnetic induction intensity on z direction of the points. Moreover, the smaller the COV value is, the better the uniformity is.

Equation (5) shows that B_z is a function of radius, turns, and other parameters. In the follow-up study, the maximum outer radius of the transmitting coil is set to 80 mm; the turns are set to 10 turns; the transmission distance is set to 20 mm.

Therefore, the radius of each turn of the transmitting coil should meet the following conditions.

$$0 < R_{i-1} < R_i \leq 80 \tag{8}$$

4.3. Genetic Algorithm Optimization

The optimized process is shown in Figure 11. The specific steps are as follows:

Firstly, the parameter R_i is binary coded to generate an initial population. Secondly, the parameters are processed; the objective function value is calculated; whether the constraint conditions are violated is judged. Thirdly, the algorithm judges whether the cutoff condition is satisfied or not. Namely, the algorithm judges whether the rate of change of the objective function is less than 10-6 or not. If it is satisfied, the objective

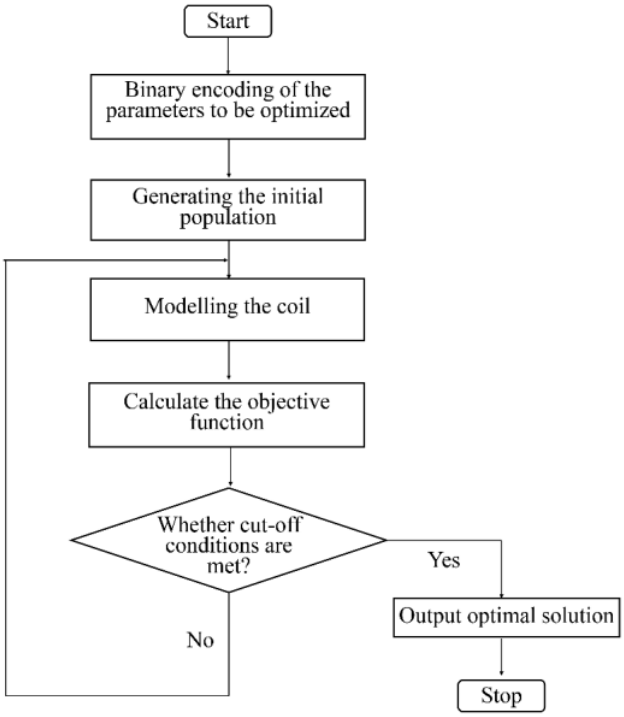

FIGURE 11. The optimized process.

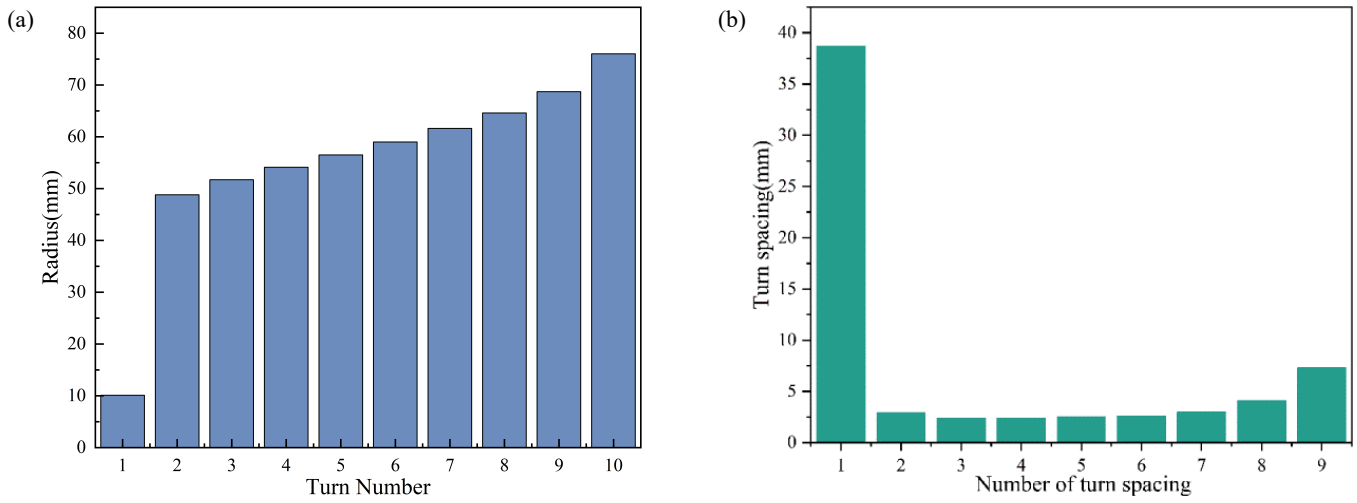

FIGURE 12. The optimized result. (a) Radius of each turn of the coil; (b) The spacing of each turn.

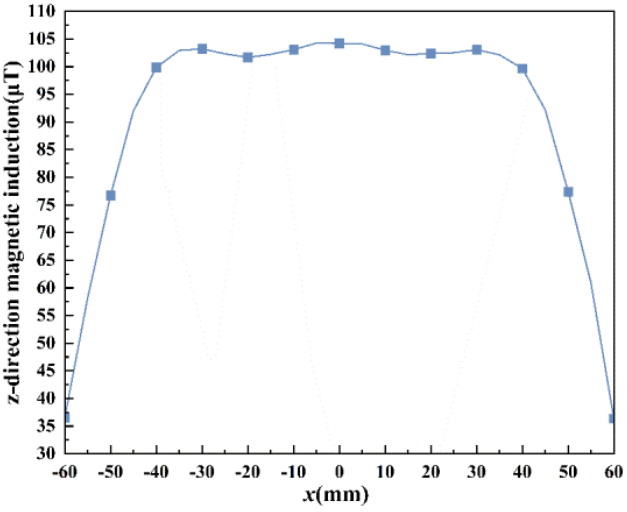

FIGURE 13. Trends in Z-direction magnetic inductance.

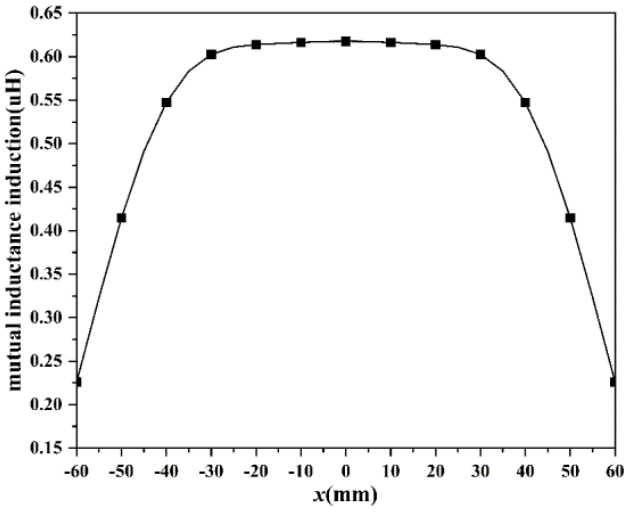

FIGURE 14. Trends in mutual inductance induction distribution.

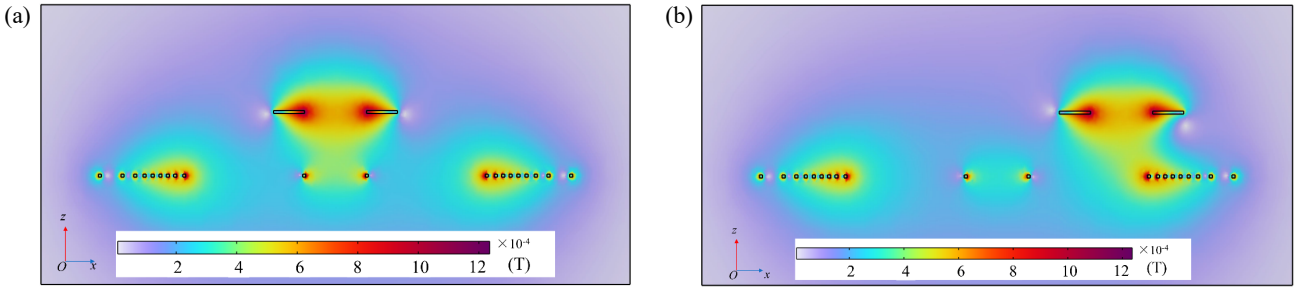

FIGURE 15. Magnetic induction intensity distribution of the optimized coupling mechanism. (a) offset distance = 0 mm and (b) offset distance = 40 mm.

function k is selected as the optimal individual; the optimal solution is compiled; the algorithm comes to an end. If not, the algorithm carries out three genetic operator operations including crossover, variation, and selection. After that, the algorithm calculates the objective function and other operations again until the cutoff condition is satisfied.

The last is that the algorithm finally outputs the optimal solution.

Figure 12(a) shows the optimization results of the radius of each turn of the transmitting coil. The inner diameter and outer diameter are 10 mm and 76 mm, respectively. Figure 12(b) shows the spacing of each turn of the optimized coil. The spac-

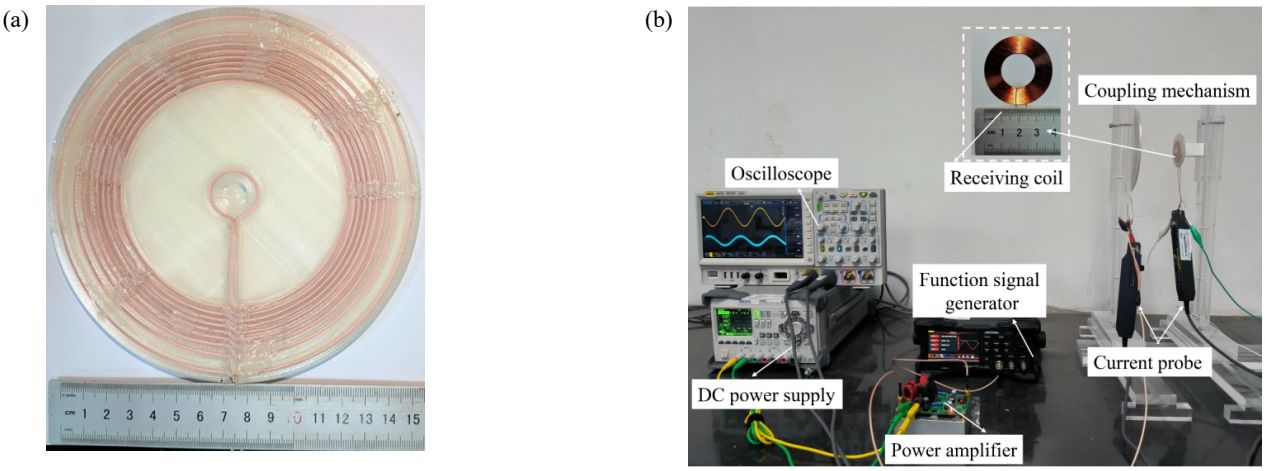

FIGURE 16. (a) Optimized transmitting coil; (b) Experimental platform.

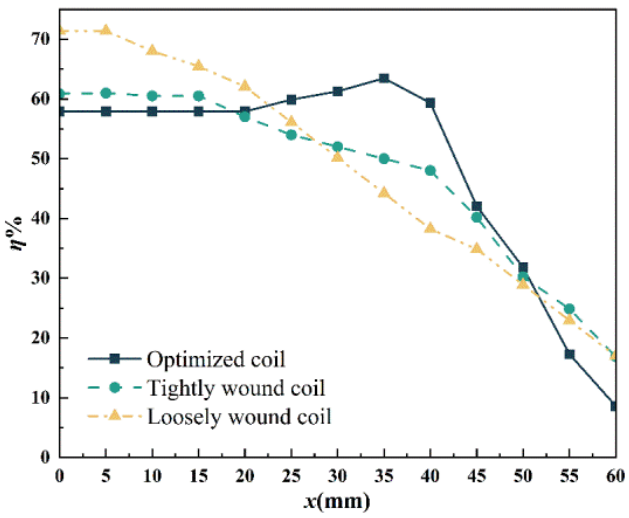

FIGURE 17. Trend of system efficiency with different transmitting coils.

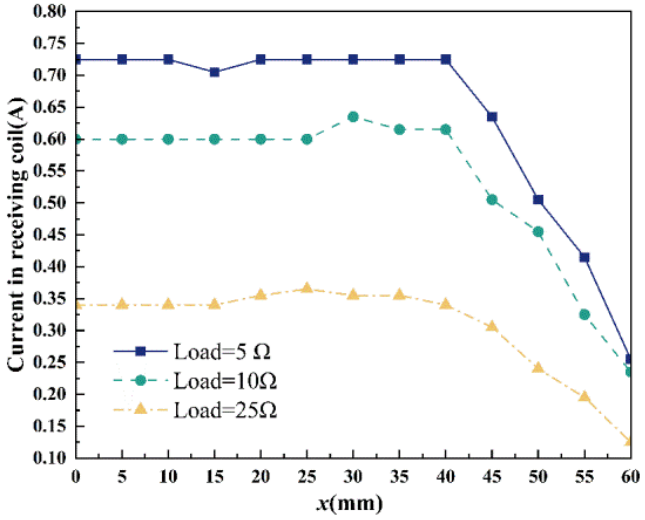

FIGURE 18. Trend of current under offset condition.

ing between the first and second turns is large, while the spacing between the second and seventh turns is smaller and more uniform, which is very consistent with the analysis in Section 3. The second to seventh turns are equivalent to tightly wound coils, while the first turn makes up the defect that the magnetic induction intensity in the center of tightly wound coils is small, so the optimization result is in line with the theoretical prediction.

Figure 13 shows the trend of the distribution of the magnetic induction intensity at the optimization plane after the optimization by using GA. The optimized coil produces a more uniform magnetic induction intensity at the optimization region than the traditional disk coil.

Figure 14 shows the trend of mutual inductance of the coupling system under offset working condition after the optimization of the transmitter coil. The abscissa represents the distance of lateral offset of the receiving coil. The mutual inductance keeps relatively constant in the range of $[-40, 40]$ mm for the coil offset position.

The distributions of the magnetic induction intensity of the optimized asymmetric coupling system is shown in Figure 15. Figure 15(a) is the situation that the receiving coil is coaxial with the transmitting coil, and Figure 15(b) is the situation that the receiving coil is offset, and the magnetic induction intensity distribution in the center of the coupling system is more uniform than that before optimization shown in Figure 6. When the receiving coil is offset by 40 mm, the distribution of the magnetic induction intensity between the coupling system is close to that when the offset has not occurred.

Figures 14 and 15 prove the uniformity of the mutual inductance and the magnetic field. It has been clarified in the previous section that the mutual inductance of the coupling system and the degree of uniformity of the spatial magnetic field are the key factors in determining the transmission efficiency of the WPT system. Therefore, the optimized coupling system possesses a uniform spatial magnetic induction intensity distribution, and the stability of the mutual inductance under the offset condition can enhance the system's anti-offset ability.

5. EXPERIMENT VERIFICATION

5.1. Experiment Platform

In order to verify the effectiveness of the proposed asymmetric coupling system and its coil parameter GA optimization method, an experiment platform shown in Figure 16 is constructed.

The proposed optimized transmitting coil is winding on a fabrication coil skeleton whose parameters are according to the optimized results. The experiment platform consists of the proposed coupling system, a DC power supply, a power amplifier, and resonance compensation capacitors. The working state is that the system maintains a constant output current of 1A and a resonant frequency of 1.5 MHz. The specific parameters of the experiment are shown in Table 2.

TABLE 2. Parameters of the experiment.

Parameters	Transmitting coil	Receiving Coil
Turns	1	28
External diameter/mm	152	4
Wire diameter/mm	1	.35
Self-inductance/μH	14.6	29.5
Compensation capacitor/pF	771	382

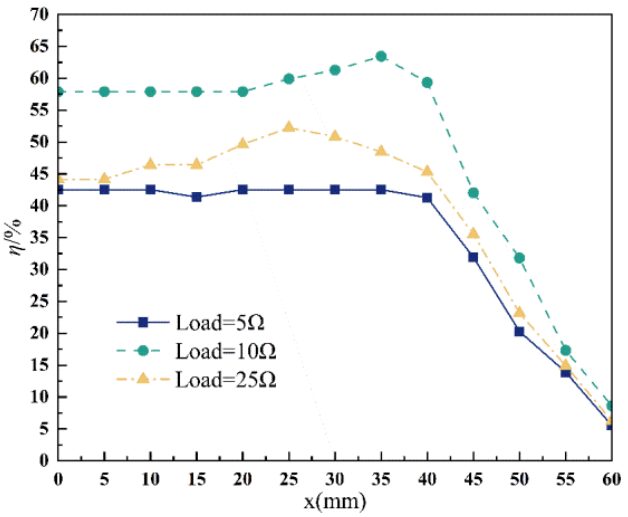

FIGURE 19. Trends of efficiency under offset condition.

5.2. Analysis of Experimental Results

Figure 17 shows the trend of system efficiency with offset distance when different transmitting coils are used, and the load is 10 Ω. The result shows that the transmission efficiency of WPT system with non-optimized transmitting coil is higher than that of WPT system with optimized transmitting coil when the offset distance is 0, because the non-optimized transmitting coil has larger self-inductance coefficient, and the mutual inductance between non-optimized transmitting coil and receiving coil is greater. However, with the increase of offset distance, the efficiency of WPT system with non-optimized transmitting coil decreases gradually, while the WPT system with optimized transmitting coil can keep its efficiency stable in a certain range.

Figures 18 and 19 show the trend of the receiving coil current and the system transmission efficiency of the experimental WPT system under the offset condition, respectively. Figure 18 shows that the current in the receiving coil can remain relatively stable in the range of [0, 40] mm after the receiving coil is offset, and the maximum current in the coil decreases with the increase of load. The result proves that the proposed the coupling system possesses ability of keeping the current stable.

Figure 19 shows the trend of the system efficiency after the receiving coil is offset, which proves that the optimized coupling system can keep the system efficiency constant within a certain range under the offset condition. The maximum efficiency of the system shows a tendency of increasing and then decreasing with the increase of the load.

The experimental results show that the asymmetric coupling system and its GA optimization method proposed in this paper can improve the anti-offset ability of WPT system and keep the WPT system running stably within a certain offset range.

6. CONCLUSIONS

In this paper, a WPT system with asymmetric coupling mechanism is investigated. A planar disk-type asymmetric coupling system is proposed, and the turn spacing of the transmitting coil is optimized by a GA optimization algorithm. The proposed coupling system and the proposed GA are verified by an experiment. The result shows that the WPT can be operated stably under the offset working condition, which may meet the requirement of implantable medical device. The main contributions of this paper are as follows:

1) An asymmetric WPT system of coupling mechanism is analyzed by circuit theory and electromagnetic theory, and the factors affecting the efficiency of the system are obtained.

2) The effects of different coil structures on the spatial magnetic induction intensity distribution of the coupling system are found.

3) A new type of coil is proposed on the basis of the traditional coil structure and optimized by the GA.

4) Finally, the feasibility of the proposed structure and the optimization method is verified by an experiment.

In the future, the coupling system could be optimized via the proposed method according to other size restricted situations.

ACKNOWLEDGEMENT

This work was supported financially by the National Natural Science Foundation of China (Grant No. 52007159), and the Natural Science Foundation of Southwest University of Science and Technology (Grant No. 20zx7116).

REFERENCES

[1] Song, M., P. Jayathurathnage, E. Zanganeh, M. Krasikova, P. Smirnov, P. Belov, P. Kapitanova, C. Simovski, S. Tretyakov, and A. Krasnok, "Wireless power transfer based on novel physical concepts," *Nature Electronics*, Vol. 4, No. 10, 707–716, Oct. 2021.

[2] Huang, X., W. Wang, and L. Tan, "Technical progress and application development of magnetic coupling resonant wireless power transfer," *Automation of Electric Power Systems*, Vol. 41, No. 2, 2–14+141, 2017.

[3] Kang, J., D. Zeng, J. Lu, and X. Shi, "Analysis of the magnetic field magnetoinductive wave characteristics of a wireless power transfer system," *Sensors*, Vol. 22, No. 24, Dec. 2022.

[4] Mapara, S. and V. Patravale, "Medical capsule robots: a renaissance for diagnostics, drug delivery and surgical treatment," *Journal of Controlled Release*, Vol. 261, 337–351, Sep 10, 2017.

[5] Lu, X., P. Wang, D. Niyato, D. Kim, and Z. Han, "Wireless charging technologies: Fundamentals, standards, and network applications," *IEEE Communications Surveys and Tutorials*, Vol. 18, No. 2, 1413–1452, 2016.

[6] Kang, J., J. Lu, D. Zeng, and X. Shi, "Analysis on the spatial impedance of the wireless power transfer system in the near field," *Progress in Electromagnetics Research C*, Vol. 123, 101–116, 2022.

[7] Zhang, J., R. Das, J. Zhao, N. Mirzai, J. Mercer, and H. Heidari, "Battery-free and wireless technologies for cardiovascular implantable medical devices," *Advanced Materials Technologies*, Vol. 7, No. 6, 201086, 2021.

[8] Khan, S., S. Pavuluri, G. Cummins, and M. Y., "Wireless power transfer techniques for implantable medical devices: a review," *Sensors*, Vol. 20, No. 12, Jun. 2020.

[9] Khan, N., H. Matsumoto, and O. Trescases, "Wireless electric vehicle charger with electromagnetic coil-based position correction using impedance and resonant frequency detection," *IEEE Transactions on Power Electronics*, Vol. 35, No. 8, 7873–7883, Aug. 2020.

[10] Kadem, K., F. Benyoubi, M. Bensetti, Y. Le Bihan, E. Laboure, and M. Debbou, "An efficient method for dimensioning magnetic shielding for an induction electric vehicle charging system," *Progress in Electromagnetics Research-pier*, Vol. 170, 153–167, 2021.

[11] Li, Z., Z. Chen, J. Li, and et al., "Coupling coefficient calculation of arbitrarily positioned rectangular coils with double magnetic shielding in wireless power transfer systems," *Progress in Electromagnetics Research B*, Vol. 98, 39–57, 2023.

[12] Li, Z., J. Li, J. Yi, W. Liao, and M. Zhang, "Optimization of quasi-constant mutual inductance of asymmetrical coils with lateral misalignment in wireless power transfer system," *Progress in Electromagnetics Research M*, Vol. 86, 103–114, 2019.

[13] Jia-Hui, Z., G. Qiang, L. Qi, F. Wei, and P. Jia-Yu, "Design and parameter optimization on coupling coil in wireless power transfer system via magnetic resonance," *Advanced Technology of Electrical Engineering and Energy*, Vol. 51, No. 24, 57–62, 2021.

[14] Bouanou, T., H. El Fadil, A. Lassioui, O. Assaddiki, and S. Njili, "Analysis of coil parameters and comparison of circular, rectangular, and hexagonal coils used in wpt system for electric vehicle charging," *World Electric Vehicle Journal*, Vol. 12, No. 1, Mar. 2021.

[15] Seo, D.-W. and S. Njili, "Comparative analysis of two- and three-coil wpt systems based on transmission efficiency," *IEEE Access*, Vol. 7, 151 962–151 970, 2019.

[16] Zhang, B., Q. Chen, L. Zhang, J. Chen, L. Xu, X. Ren, and Z. Zhang, "Triple-coil-structure-based coil positioning system for wireless ev charger," *IEEE Transactions on Power Electronics*, Vol. 36, No. 12, 13 515–13 525, Dec. 2021.

[17] Seshadri, S., M. Kavitha, and P. Bobba, "Effect of coil structures on performance of a four-coil wpt powered medical implantable devices," in *2018 International Conference on Power, Instrumentation, Control and Computing (PICC)*, Thrissur, India, 1–6.

[18] Elliott, G. J., S. Raabe, G. Covic, and J. Boys, "Multiphase pickups for large lateral tolerance contactless power-transfer systems," *IEEE Transactions on Industrial Electronics*, Vol. 57, No. 5, 1590–1598, May. 2010.

[19] Chen, Y., T. Tang, J. Chen, and et al., "Optimization design of multi-receiver wireless power transfer system based on a spherical coil," *Engineering Journal of Wuhan University*, Vol. 55, No. 5, 503–509, 2022.

[20] Bilandzija, D., D. Vinko, and M. Barukcic, "Genetic-algorithm-based optimization of a 3d transmitting coil design with a homogeneous magnetic field distribution in a wpt system," *Energies*, Vol. 15, No. 4, Feb. 2022.

[21] Noda, T., T. Nagashima, X. Wei, M. Kazimierczuk, and H. Sekiya, "Design procedure for wireless power transfer system with inductive coupling-coil optimizations using pso," in *2016 IEEE International Symposium on Circuits and Systems (ISCAS)*, 646–649, iEEE International Symposium on Circuits and Systems (ISCAS), Montreal, Canada, May 22-25, 2016.

[22] Tan, P., W. Xu, X. Shangguan, and et al., "Mutual inductance modeling and parameter optimization of wireless power transfer system with combined series-wound hexagonal coils," *Transactions of China Electrotechnical Society*, Vol. 38, No. 9, 2299–2309, 2023.

[23] Pingan, T., L. Chunxia, Y. Liangwei, P. Tao, and G. Xieping, "Coupling mechanism analysis for multi-transmitter switching wireless power transfer system," *Transactions of China Electrotechnical Society*, Vol. 33, No. 22, 5244–5253, 2018.

[24] Wu, D., T. He, X. Wang, and Q. Sun, "Analytical modeling and analysis of mutual inductance coupling of rectangular spiral coils in inductive power transfer," *Diangong Jishu Xuebao/transactions of China Electrotechnical Society*, Vol. 33, 680–688, 02. 2018.

[25] Xiu-Quan, L., Z. Zhao-Rui, and H. Ping, "Numerical and experimental analysis on performances of coreless coil inductance," *Journal of Engineering Design*, Vol. 2, 149–153, 2008.

[26] Chao, L., Q. Hong, X. Yang, and et al., "Numerical simulation of magnetic field distribution and magnetic field lines of ring-like current based on c++," *Physical Experiment of College*, Vol. 34, No. 3, 28–30, 2021.